

See discussions, stats, and author profiles for this publication at: <https://www.researchgate.net/publication/261568121>

Cover Picture: Conformational Dynamics of DNA G-Quadruplex in Solution Studied by Kinetic Capillary Electrophoresis Coupled On-line with Mass Spectrometry (ChemistryOpen 2/2014)

ARTICLE *in* CHEMISTRYOPEN · APRIL 2014

Impact Factor: 3.25 · DOI: 10.1002/open.201400004

READS

34

5 AUTHORS, INCLUDING:



Gleb G Mironov

University of Ottawa

14 PUBLICATIONS 67 CITATIONS

[SEE PROFILE](#)



Victor Okhonin

Custoimetrics Inc.

68 PUBLICATIONS 825 CITATIONS

[SEE PROFILE](#)

DOI: 10.1002/open.201400002

Conformational Dynamics of DNA G-Quadruplex in Solution Studied by Kinetic Capillary Electrophoresis Coupled On-line with Mass Spectrometry**

Gleb G. Mironov, Victor Okhonin, Nasrin Khan, Christopher M. Clouthier, and Maxim V. Berezovski^{*[a]}

G-quadruplex-forming DNA/RNA sequences play an important role in the regulation of biological functions and development of new anticancer and anti-aging drugs. In this work, we couple on-line kinetic capillary electrophoresis with mass spectrometry (KCE-MS) to study conformational dynamics of DNA G-quadruplexes in solution. We show that peak's shift and its widening in KCE can be used for measuring rate and equilibrium constants for DNA–metal affinity interactions and G-quadruplex formation; and ion mobility mass spectrometry (IM-MS) provides information about relative sizes, absolute molecular

masses and stoichiometry of DNA complexes. KCE-MS separates a thrombin-binding aptamer d[GGTTGGTGTGGTTGG] from mutated sequences based on affinity to potassium, and reveals the apparent equilibrium folding constant ($K_f \approx 150 \mu\text{M}$), folding rate constant ($k_{on} \approx 1.70 \times 10^3 \text{ s}^{-1} \text{ M}^{-1}$), unfolding rate constant ($k_{off} \approx 0.25 \text{ s}^{-1}$), half-life time of the G-quadruplex ($t_{1/2} \approx 2.8 \text{ s}$), and relaxation time ($\tau \approx 3.9 \text{ ms}$ at physiological 150 mM [K⁺]). In addition, KCE-MS screens for a GQ-stabilizing/-destabilizing effect of DNA binding dyes and an anticancer drug, cisplatin.

Introduction

G-quadruplexes (GQs) are noncanonical secondary structures formed from G-rich sequences of nucleic acids, and play important roles in the regulation of gene transcription and translation. Formation of GQs in a telomere region causes inhibition of telomerase activity with subsequent obsolescence and cell death.^[1] GQ structures are found in some promoters of oncogenes, such as c-MYC,^[2] BCL-2,^[3] c-KIT,^[4] K-ras,^[5] VEGF.^[6] Therefore, GQs could be a key therapeutic target for anticancer drugs. Quarroxin, a GQ-stabilizing drug for the treatment of neuroendocrine/carcinoid tumors has reached phase II clinical trials.^[7] Recently, a novel translation activation function of GQs in 3'-untranslated regions (3'-UTR) of messenger RNAs was also presented.^[8]

While the idea of GQ-stabilizing/-destabilizing compounds looks promising for switching genes on and off, it is critical to

measure kinetics of GQ folding in solution for efficient drug design and high-throughput screening of drug candidates. Finding kinetic parameters can relate the GQ folding time scale with biological processes like replication and transcription. Up to now, the most common techniques for studying of GQ conformations include circular dichroism (CD),^[9] UV absorption at 295/297 nm,^[10] non-denaturing gel electrophoresis,^[11] fluorescence-based single molecule methods,^[12] nuclear magnetic resonance (NMR),^[13] surface plasmon resonance (SPR)^[14] and X-ray crystallography (XRC).^[15] However, standalone CD studies the conformational changes in anisotropic molecules and chiral super assemblies in equilibrium, and for fast interactions it measures thermodynamic constants only. NMR shows the DNA's conformational dynamic in solution with atomic resolution. XRC provides a static picture of a DNA conformation. Alternatively, fluorescence resonance energy transfer (FRET)^[16,17] measures the relative distance between fluorescent residues or labels and requires fluorescent labeling that may interfere with DNA dynamics and ligand binding. The main disadvantages of NMR techniques are a requirement for the high concentration of a sample (around millimolar range) and difficulties in performing a multiplex study. Other solution-based techniques do not provide direct information about the structure of a GQ, making it challenging to interpret the data. The main methods for measuring kinetics of DNA folding and affinity binding are stopped-flow (SF)^[10] and SPR,^[14] both of which have the capability of calculating rate and thermodynamic constants of DNA binding to big biomolecules. They have restrictions due to mixing dead-time and re-dissociation of reagents for SF as well as mass transport to and heterogeneity of the surface of a SPR chip.

[a] G. G. Mironov, Dr. V. Okhonin, Dr. N. Khan, Dr. C. M. Clouthier, Prof. Dr. M. V. Berezovski

Department of Chemistry, University of Ottawa
10 Marie Curie, Ottawa K1N 6N5 (Canada)
E-mail: maxim.berezovski@uottawa.ca

[**] This article is part of the Virtual Special Issue "Structure Characterization of Biomolecules"

Supporting information for this article is available on the WWW under <http://dx.doi.org/10.1002/open.201400002>. Supporting Information contains detailed analytical mathematical solutions for fast kinetics, cisplatin derivatization of GQ and GM.

© 2014 The Authors. Published by Wiley-VCH Verlag GmbH & Co. KGaA. This is an open access article under the terms of the Creative Commons Attribution-NonCommercial-NoDerivs License, which permits use and distribution in any medium, provided the original work is properly cited, the use is non-commercial and no modifications or adaptations are made.

In this article, we demonstrate the power of kinetic capillary electrophoresis coupled on-line with mass spectrometry (KCE-MS) to monitor individual DNA conformers and revealing rate and equilibrium constants of GQ DNA folding upon the binding to potassium ions. This represents an important step in deciphering fast kinetics of DNA folding, in addition to establishing KCE-MS as a real-time method for studying DNA dynamics and screening DNA binding ligands.

Conceptually, KCE-MS is defined as an electrophoretic separation of compounds, which interact inside a capillary column during electrophoresis and are detected by mass spectrometry. Usually, separated analytes are detected by UV-VIS absorption or laser-induced fluorescence (LIF). These detection modes can be problematic for screening of complex mixtures with multiple targets and ligands. Therefore, the ability to acquire accurate molecular mass and structural information about the analytes is highly desirable. Capillary electrophoresis was coupled with mass spectrometry (CE-MS) over twenty years ago, which significantly advanced the field of nucleic acid and bioanalytical chemistry.^[18] Here, we connect KCE with MS on-line by electrospray ionization (ESI), a soft ionization technique, which keeps noncovalent complexes intact. It combines in one system the separation and kinetic capability of KCE together with molecular weight and structural elucidation of MS. The advantages of KCE-MS are that 1) DNA interacts with a ligand and folds at near physiological conditions, and all kinetic and thermodynamic parameters are measured in solution but not a gas phase; 2) DNA and ligands don't need special labeling for the MS detection; and 3) interactions/foldings of several DNAs and ligands can be studied simultaneously in one capillary microreactor. KCE-MS implicates the benefits of both ion mobility, mass spectrometry and KCE-UV(LIF), where ion intensities, masses, electrophoretic mobilities and affinity of interacting compounds are determined. Ion mobility (IM) spectrometry separates ions on the basis of their collision cross section with a buffer gas. IM is fast and simple, and requires only a MS instrument with a drift cell. Nevertheless, the competitive binding, ion suppression during ionization and formation of non-specific complexes in a gas phase could cause problems in interpretation of IM results. Fortunately, KCE can be coupled with IM directly, so that KCE separates interacting molecules based on their affinities and size-to-charge ratios in solution inside a capillary prior to the electrospray ionization (ESI), followed by IM separation in a gas phase and MS detection.

Results and Discussion

Principles of KCE

KCE-based separation of GQ DNA involves two major processes. First, it includes the noncovalent interaction of an unfolded DNA (DNA) with a coordinating metal ion (M) leading to formation of a folded GQ complex (GQ-M) and dissociation of the complex regulated by a rate constant of complex formation (k_{on}) and a decay constant (k_{off}) [Eq. (1)]:



Second, there is simultaneous separation of DNA, M, and GQ-M based on differences in their electrophoretic velocities in solution. These velocities are directly proportional to a size/charge ratio of DNA, M, and GQ-M. These two processes are described by the reaction scheme shown in Equation (1) and general system of partial differential Equation (2):

$$\begin{aligned} & \frac{\partial[\text{DNA}]}{\partial t} + V_{\text{DNA}} \frac{\partial[\text{DNA}]}{\partial x} - D_{\text{DNA}} \frac{\partial^2[\text{DNA}]}{\partial x^2} \\ &= \frac{\partial[\text{M}]}{\partial t} + V_{\text{M}} \frac{\partial[\text{M}]}{\partial x} - D_{\text{M}} \frac{\partial^2[\text{M}]}{\partial x^2} \\ &= - \frac{\partial[\text{GQ} - \text{M}]}{\partial t} - V_{\text{GQ-M}} \frac{\partial[\text{GQ} - \text{M}]}{\partial x} + D_{\text{GQ-M}} \frac{\partial^2[\text{GQ} - \text{M}]}{\partial x^2} \\ &= k_{off}[\text{GQ} - \text{M}] - k_{on}[\text{DNA}][\text{M}] \end{aligned} \quad (2)$$

where $[\text{DNA}]$, $[\text{M}]$ and $[\text{GQ}-\text{M}]$ are the concentrations of a unfolded DNA, metal ion, and a folded GQ-metal complex, respectively, V_{DNA} , V_{M} and $V_{\text{GQ-M}}$ are the migration velocities, D_{DNA} , D_{M} and $D_{\text{GQ-M}}$ are the diffusion coefficients, t is the time, x is the spatial coordinate along a capillary.

Practically, a plug of an equilibrium mixture (EM) that consists of DNA, M, and GQ-M is injected into the capillary pre-filled with the run buffer containing the metal ion with a total concentration identical to EM. Components of EM are separated by capillary electrophoresis while quasi-equilibrium is maintained between DNA, M and GQ-M complex inside the capillary (Figure 1 A). This method is called equilibrium capillary electrophoresis of equilibrium mixtures (ECEEM).^[19] It is a mode of kinetic capillary electrophoresis (KCE), a platform for kinetic homogeneous affinity methods in which molecules interact with each other during electrophoretic separation.^[20] The unfolded DNA and folded GQ migrate with different velocities due to different shapes—GQ is more compact than unfolded DNA (Figure 1 B), and thus migrates later than the unfolded DNA. There are three unique features of this separation: 1) DNA and GQ migrate as a single EM peak due to fast exchange between them, 2) the migration time of the EM peak depends on the concentration of M in the run buffer, so DNA sequences with different equilibrium folding constants, $K_F = k_{off}/k_{on}$, migrate with different velocities and are separated from each other, and 3) EM peak broadening is dependent on the concentration of M, rate constants and characteristic separation time (t_{sep}). The characteristic separation time is the time required for DNA and GQ-M to separate from each other inside EM plug and is defined as [Eq. (3)]:

$$t_{sep} = w / (2|V_{\text{GQ-M}} - V_{\text{DNA}}|) \quad (3)$$

where w is the width of the initial EM peak.

The general analytical solution of these nonlinear differential Equations (2) in partial derivatives is not known. In some cases like 1) the formation or decay rate constants are negligible or zero,^[21,22] 2) $V_{\text{GQ-M}} = V_{\text{M}}$ or $V_{\text{GQ-M}} = V_{\text{DNA}}$, Equations (2) become

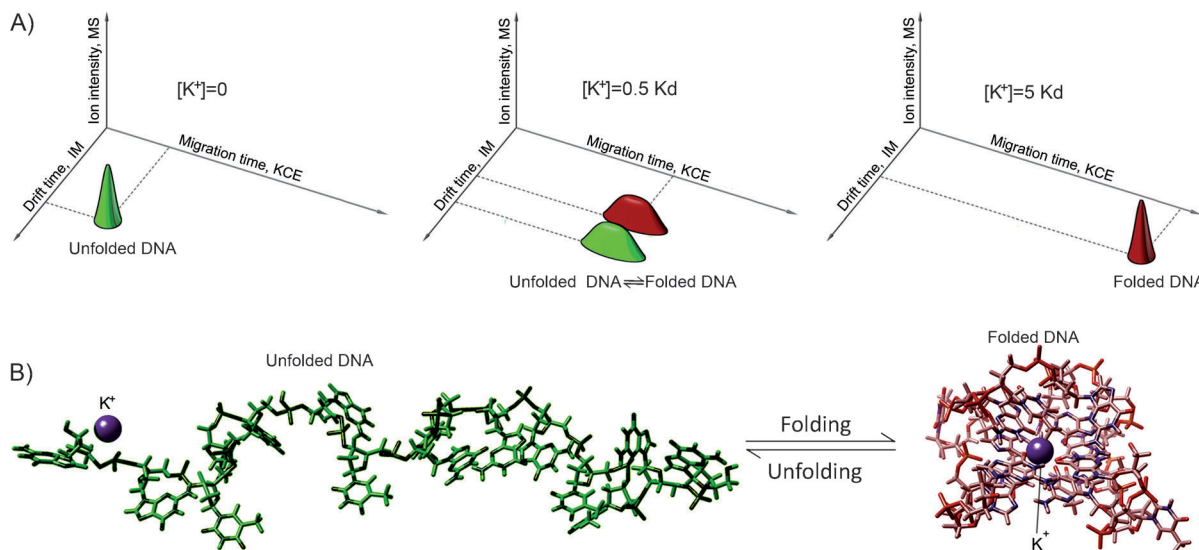


Figure 1. Schematic representation of two-dimensional separation (KCE versus IM) of unfolded (green) and folded (red) forms of GQ DNA. A) First dimension is KCE separation in solution; the second dimension is IM separation in a gas phase. B) DNA folding in a compact GQ structure is mediated by potassium ion.

linear directly or after the Cole–Hopf substitution.^[23,24] In our case, the molecular exchange between an unfolded DNA and a folded GQ-M complex is very fast. The relaxation time (τ) to equilibrium for weak ($K_F > 1 \mu\text{M}$) and fast reactions depends on rate constants, DNA and M concentrations [Eq. (4)]:

$$\tau = 1/(k_{\text{on}}([DNA] + [M]) + k_{\text{off}}) \quad (4)$$

If $\tau > t_{\text{sep}}$, the zones of DNA and GQ-M are separated before the re-equilibration in Equation (1) proceeds to a significant extent. Thus, unfolded DNA and folded GQ-M are moving as individual peaks. If $\tau \approx t_{\text{sep}}$, re-equilibration in Equation (1) and separation proceed with comparable rates. Therefore, DNA and GQ-M are moving as two overlapping peaks. Finally, if $\tau < t_{\text{sep}}$, the re-equilibration in Equation (1) occurs much faster than peak separation (our case), and, as a result, DNA and GQ-M will be moving as a single peak. The last case of fast molecular interactions is experimentally illustrated in Figure 2.

For the fast molecular exchange, when $\tau \ll t_{\text{sep}}$ and $[DNA] \ll [M] + K_F$, the approximated Equation (5) is used:

$$\begin{aligned} \partial_t [DNA] + \left(V_{\text{EM}} - \frac{2k_{\text{off}} D_{\text{CID}}}{K_F(V_{\text{DNA}} - V_{\text{EM}})} [DNA] \right) \partial_x [DNA] \\ \approx (D_{\text{CID}} + D_{\text{EM}}) \partial_x^2 [DNA] \end{aligned} \quad (5)$$

where V_{EM} is the velocity of the EM peak, D_{EM} is a physical diffusion coefficient for the EM peak and D_{CID} is a chemical induced coefficient of diffusion. They can be described as [Eq. (6)]:

$$V_{\text{EM}} \equiv \frac{K_F V_{\text{DNA}} + [M] V_{\text{GQ-M}}}{K_F + [M]} \quad (6a)$$

$$D_{\text{EM}} \equiv \frac{K_F D_{\text{DNA}} + [M] D_{\text{GQ-M}}}{K_F + [M]} \quad (6b)$$

$$D_{\text{CID}} \equiv \frac{[M] K_F^2 (V_{\text{GQ-M}} - V_{\text{DNA}})^2}{k_{\text{off}} (K_F + [M])} \quad (6c)$$

K_F can be found from the expression:

$$K_F \approx \sum_i \frac{(V_{\text{EM}}^i - V_{\text{DNA}})^3 (V_{\text{GQ-M}} - V_{\text{EM}}^i)}{[M]_i} / \sum_i \frac{(V_{\text{EM}}^i - V_{\text{DNA}})^4}{[M]_i^2} \quad (7)$$

Equation (5) is well known in mathematics as Burgers' equation and can be solved analytically if the injected EM plug is narrow ($w \ll$ the length of capillary).^[25] The detailed mathematical solution is described in the Supporting Information. When V_{DNA} , $V_{\text{GQ-M}}$, V_{EM} , $D_{\text{GQ-M}}$, D_{DNA} are known, K_F is found from Equation (7). Afterward, k_{off} is determined from Equation (5), and $k_{\text{on}} = k_{\text{off}}/K_F$. Interesting to note, ECEEM has a unique "accumulation" property. It accumulates the effect of molecular interactions in extra-long capillaries; it could reveal rates of extremely fast reactions, if $D_{\text{CID}} > D_{\text{EM}}$.

Measuring rate and equilibrium constants for GQ folding

We mixed 10 μM of GQ, forming a 15-nucleotide (nt) thrombin-binding aptamer (TBA) sequence (5'-d[GGTTGGTGTGGTGG]-3') with three mutated sequences (10 μM each, the flipped bases are italic), GM1 (d[G^{GT}GTTGGTGT-G^{GT}GTG]), GM2 (d[G^{GT}GTTGTGGTGGTGTG]), GM3 (d[G^{GT}GTG-TGGGTGTG]) (equimolar mixture of GM1, GM2 and GM3 is labeled as GM), and separated in varying K^+ concentrations from 10 μM to 2.5 mM KCl in 12.5 mM tris-acetate (TA) run buffer, pH 7.8. All DNA sequences have the same number of nucleotides and molecular mass (MW = 4726.1 Da). As shown in Figure 2, the GQ sequence is separated well from a mixture

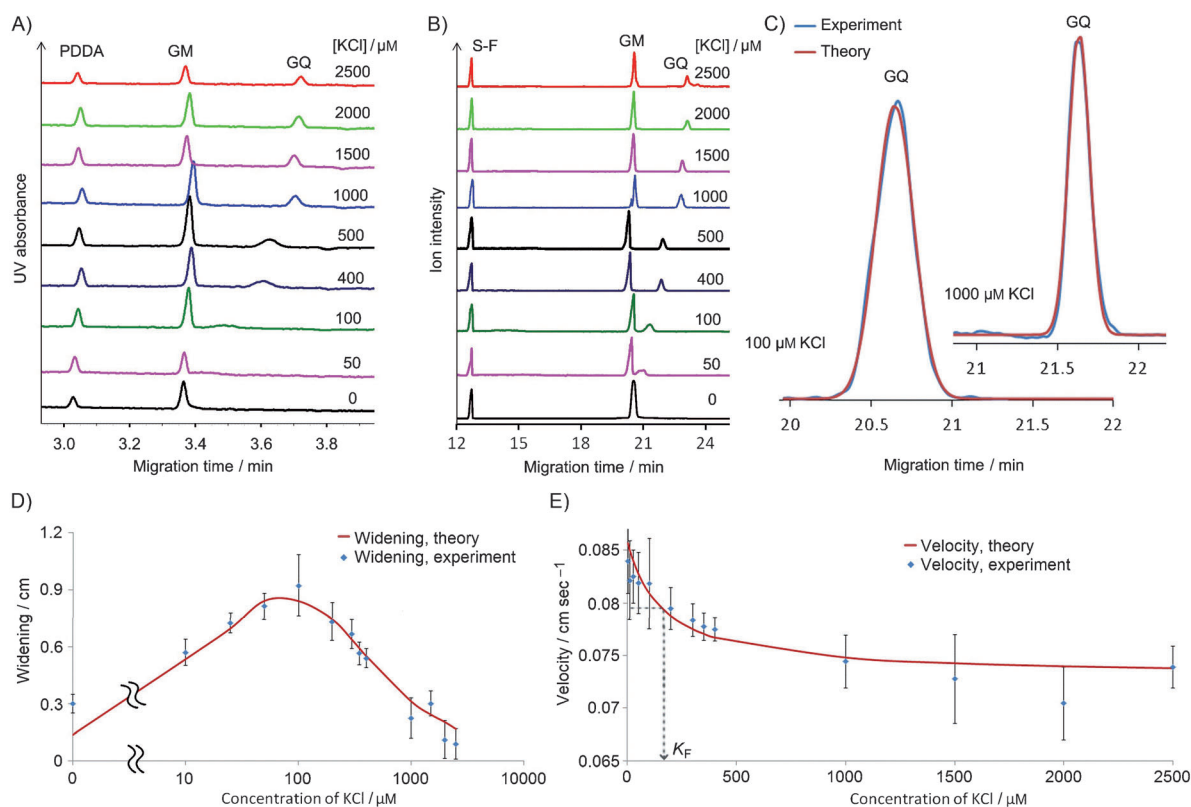


Figure 2. KCE-MS experiments for finding rate and equilibrium constants. Representative ECEEM electropherograms of four DNA strands (GM1, GM2, GM3 and GQ, 10 μ M each) and varying concentration of KCl with A) UV-detection and B) MS detection. C) Representative shapes of a GQ peak at different concentrations of KCl with MS detection. D) Dependence of GQ peak widening on the concentration of KCl with MS detection. E) Plot of GQ peak velocity as a function of KCl concentration for K_F determination with MS detection. Theoretical fitting is shown as a red curve, experimental data as blue dots or a blue curve. PDDA and S-F are internal standards.

of mutated sequences upon increasing K^+ concentration and visualized by UV (Figure 2A) and MS detections (Figure 2B). Broadening of GQ peak has a bell-shaped curve, with a maximum width at approx. 150 μ M of KCl, when fractions of unfolded DNA and GQ are equal (Figure 2D). Experiments carried out in the range of 15–450 μ M of KCl, $(0.1\text{--}3)\times K_F$ provide the most confident results for finding rate and equilibrium constants. In this range, the EM contains both DNA and GQ in comparable amounts.

Molecular diffusion can contribute to peak widening in a similar way as dynamic equilibrium between different DNA conformers. Moreover, in our case, the GQ peak became narrower with increasing migration time in experiments when $[KCl] > 500 \mu\text{M}$ —the phenomenon opposite to that could be caused by diffusion. Nevertheless, we found diffusion coefficients for GQ and GM by a CE method as described elsewhere.^[26] Briefly, we measured the change of GQ and GM peak widths with and without KCl. This was achieved by first moving an analyte in one direction to pass the UV detector and record the initial peak width. The analyte was then stopped to allow for its diffusion for 40 min. Finally, the analyte was moved back passing the detector for the second time and recording the final peak width. Diffusion coefficients for GQ and GM sequences were the same and equal to $(1.4 \pm 0.1) \times 10^{-6} \text{ cm}^2 \text{ sec}^{-1}$ without KCl, and $(4.5 \pm 0.2) \times 10^{-6}$ and $(1.8 \pm 0.2) \times 10^{-6} \text{ cm}^2 \text{ sec}^{-1}$ in presence

of 2 mM KCl, respectively. The folding of DNA to a compact GQ structure decreases molecular cross section and a diffusion coefficient accordingly.

The apparent folding constant (K_F) for GQ is $(147 \pm 8) \mu\text{M}$; k_{on} is $(1.70 \pm 0.41) \times 10^3 \text{ s}^{-1} \text{ M}^{-1}$; k_{off} for unfolding is $(0.25 \pm 0.06) \text{ s}^{-1}$. Half-life time of the complex is 2.8 s; relaxation time (τ) equals 2.0 s in 150 μM KCl and 6.5 ms in 90 mM KCl. To the best of our knowledge, this is the first report on kinetic parameters for fast DNA folding/unfolding in solution measured on-line by a separation technique and mass spectrometry. To confirm the value of K_F measured by KCE-MS, we performed independent circular dichroism (CD) titration experiments and found K_F equaled $(126 \pm 4) \mu\text{M}$ for GQ–potassium complex (see the CD section in the Supporting Information). Our results are consistent as well with that reported by Zhang and Balasubramanian^[10] for the hTelo sequence (d[GGGTTAGGGTAGGGTAGGG]): $K_F = (120 \pm 20) \mu\text{M}$, $k_{on} = (0.28 \pm 0.04) \times 10^3 \text{ s}^{-1} \text{ M}^{-1}$ and $\tau = 40 \text{ ms}$ in 90 mM KCl using UV titration and stopped-flow techniques. The hTelo sequence is 21-nt long, has 3-quartet DNA G-quadruplexes and folds with a stronger positive cooperativity than TBA with 2 quartets only; therefore, hTelo has smaller K_F and k_{on} values and longer relaxation time.

While in our experimental demonstration of KCE we used an electric field, other means of inducing differential mobility can be used, like chromatography or centrifugation. An external

action used in KCE to induce the differential mobility can potentially affect the folding kinetics. We performed our KCE separation at different electric fields and found small variations of folding constants (< 20%). Nevertheless, the possibility of such an influence cannot be completely excluded and could be experimentally studied by varying an electric field and extrapolating the results to zero voltage.

Monitoring DNA folding with ion mobility MS

The challenge for MS detection is that molecular weights and *m/z* ratios of all GM and GQ DNA sequences are the same due to the same nucleotide constitution. It makes these molecules unresolvable by means of MS only. Nevertheless, the differential affinity of DNA to K^+ can be observed by direct injection mass spectrometry (DIMS). The main ions in DIMS are $(GQ-4H^+)^{4-}$ for free GQ and $(GM-4H^+)^{4-}$ for free GM (Figure 3C,A). Mixing with 2 mM KCl eliminates free GQ as well as the Na^+ adduct (Figure 3D), but brings several complexes of GQ with K^+ where $(GQ+K^+-5H^+)^{4-}$ and $(GQ+2K^+-6H^+)^{4-}$ are the main ions. The high concentration of KCl does not significantly change the amount of free GM (Figure 3B), which confirms the absence of specific affinity of GM to K^+ . In DIMS experiments, the first and second dissociation constants K_{D1} for GQ-1K and K_{D2} for GQ-2K have been previously found to be 119 μM and 556 μM , respectively.^[27] The apparent folding constant K_F obtained in solution by KCE is inherently different from the consecutive dissociation constants K_{D1} and K_{D2} deter-

mined by mass spectrometry in a gas phase, because KCE does not resolve 1:1 and 1:2 GQ-metal complexes in solution.

Complexation of GQ with two potassium ions causes GQ folding in a compact structure with smaller collision cross section (CCS) that is detectable by ion mobility spectrometry (IMS). GQ has shorter migration in CE and drift time in IMS experiments than GM sequences (Figure 4). Addition of K^+ ions to GM sequences increases a cross section and drift time as opposed to the GQ strand (Figure 4B).

We also observed that Na^+ and NH_4^+ ions possessed weaker GQ stabilizing activity than K^+ , as was previously shown.^[28] Important to note, NH_4^+ -based buffers (popular in mass spectrometry) should be avoided in studying coordinating effects of nucleic acids with different ligands due to the fact that NH_4^+ would compete with the ligands to bind to GQ making it harder to interpret experimental results.

Balthasar et al.^[29] studied complexation of TBA (GQ sequence) with NH_4^+ using IMS and found that the loss of NH_4^+ from the complex does not change the CCS of nucleic acids, meaning that free TBA and TBA- NH_4^+ complex have identical CCS's. These findings also support our conclusion that K^+ is a stronger G-quadruplex stabilizing agent.

Screening for GQ-stabilizing/-destabilizing molecules

Since GQ structures can regulate a broad spectrum of different biological processes and cancer development, it is of a great importance to search for compounds altering its stability. We tested a set of compounds that could possibly stabilize/desta-

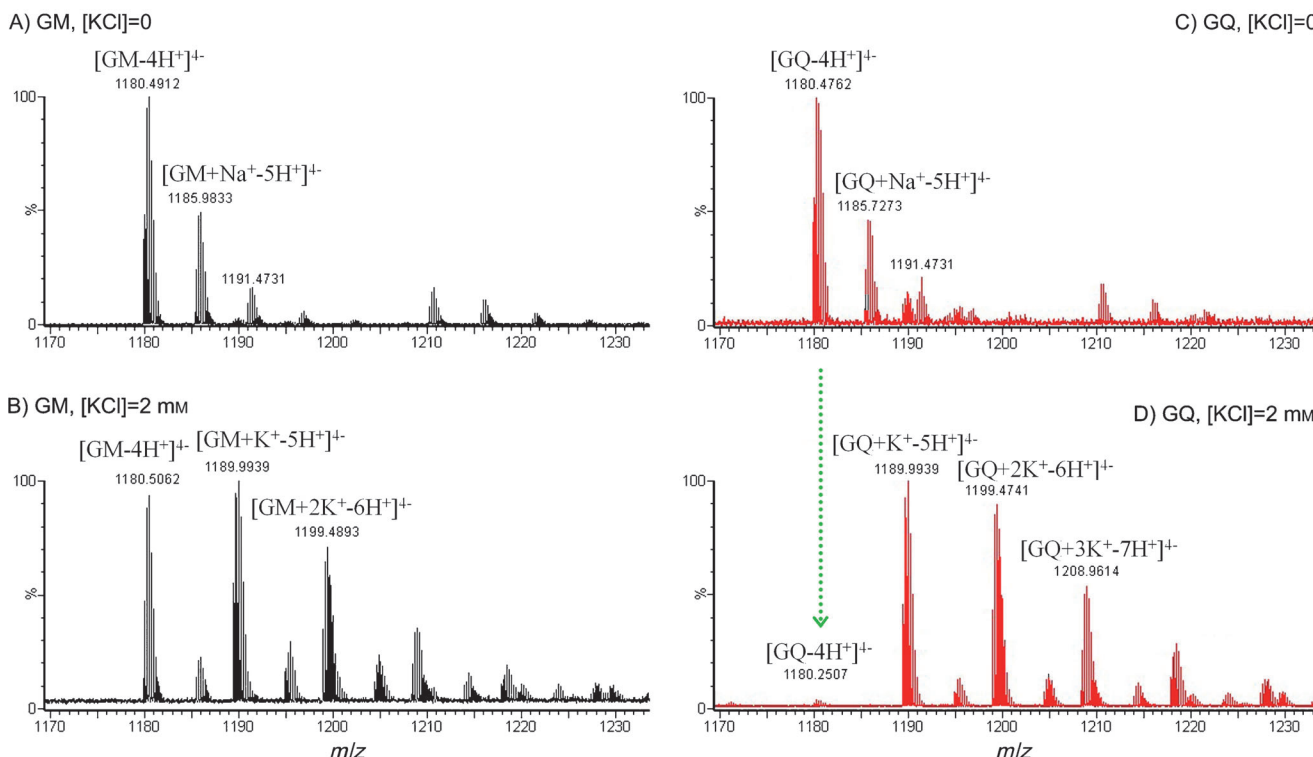


Figure 3. Ion patterns of GM (A and B) and GQ (C and D) in the absence (A, C) and presence (B, D) of KCl in DIMS. Free GQ is eliminated upon the binding with K^+ ions. GM: a mixture of GM1, GM2, GM3; GQ: a thrombin-binding aptamer.

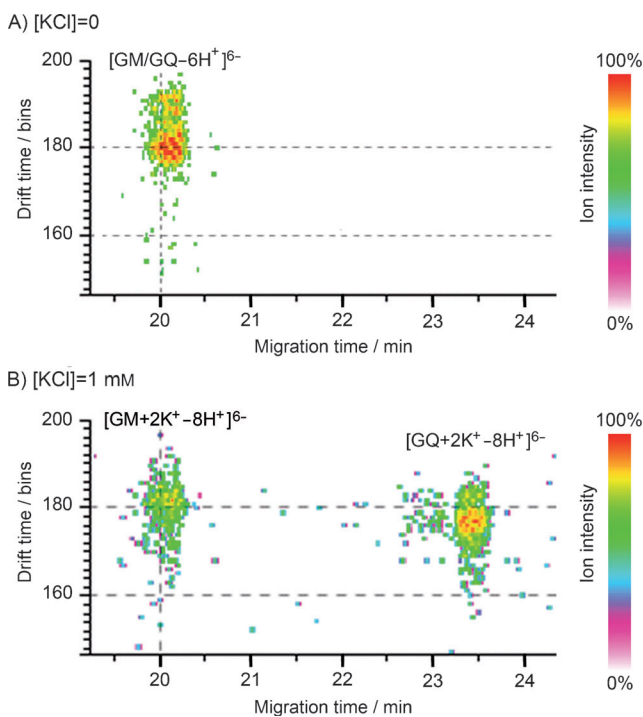


Figure 4. On-line KCE-IM-MS experiments for separation of GM (GM1, GM2 and GM3) and GQ DNA sequences. GMs and GQ are well resolved by KCE in solution and poorly resolved by IMS in the gas phase with K^+ ions (B); and are not resolved without KCl (A). Migration time relates to KCE and drift time to ion mobility spectrometry.

bilize GQ. These include nucleic acid binding dyes: SYTO, BOBO-1 iodide, BOBO-3 iodide, POPO-1 iodide, POPO-3 iodide, TOTO-1 iodide, TOTO-3 iodide, YOYO-1 iodide, YOYO-3 iodide; and an anticancer drug called cisplatin or *cis*-diamminedichloroplatinum(II). The dyes were supplemented into the run buffer as well as into samples of GQ, GM1, GM2, and GM3 sequences and were subjected to KCE-MS analysis. We did not observe any migration time shifts and peak widening in KCE, and did not detect GQ-dye complexes by MS in the range of dye concentrations from 50 nM to 1.6 μ M. We concluded that aforementioned DNA binding dyes did not possess any GQ stabilizing/destabilizing activity. Usually these dyes bind well to long double-stranded DNA.

Unlike the dyes cisplatin demonstrated strong GQ destabilizing activity. Cisplatin coordinates to the N7 atoms of the purine (guanine and adenine) bases and forms a covalent adduct with two adjacent bases on the same strand of DNA. In this experiment, GM and GQ strands were derivatized with cisplatin with and without the presence of K^+ ions (see Figure S1.2 in the Supporting Information). After derivatization, free DNA as well as monoderivatized strands were detected. Important to note, in cisplatin-DNA complexes both available bonds of cisplatin were used, which indicates intra-strand cross-linking. After cisplatin derivatization, DNA was no longer able to fold into GQ structure (see Figure S1.2D in the Supporting Information). Therefore, cisplatin could be used as a strong and nonspecific GQ-destabilizing agent.

Conclusions

Whitesides and co-authors were the first to apply CE for finding rate and equilibrium constants through a numerical approach of fitting reactant-propagation profiles.^[30,31] Most kinetic capillary electrophoresis (KCE) methods (non-equilibrium capillary electrophoresis of equilibrium mixtures (NECEEM), sweeping capillary electrophoresis (SweepCE), plug-plug KCE) cause irreversible perturbations in binding equilibrium and are not suitable for measuring reactions with fast re-equilibration ($\tau < t_{sep}$). For example, in NECEEM, if the dissociation of a complex happens quickly, it is almost impossible to measure $k_{off} > 0.1 \text{ s}^{-1}$. In contrast, equilibrium capillary electrophoresis of equilibrium mixtures (ECEEM) considers both the forward and reverse process in the reaction.

In this study, we coupled on-line kinetic capillary electrophoresis with mass spectrometry (KCE-MS) for the study of fast DNA conformations and dynamics in solution. We showed that peak's shift in CE and its widening can be used for the precise determination of rate and equilibrium constants for DNA-metal affinity interactions and DNA folding. We confirmed DNA folding by ion mobility (IM) spectroscopy and presented two-dimensional separation (KCE versus IM) of conformers in solution and a gas phase.

In conclusion, KCE-MS establishes a new paradigm that separation methods together with MS detection can be used as comprehensive kinetic tools with mass and structure elucidation of nucleic acids. Most previous attempts to use chromatography and electrophoresis for studying nucleic acid interactions were restricted to assuming slow or no equilibrium between reactants. KCE shows that non-zero kinetics and structural dynamics must be taken into account when separation happens. KCE-MS could be a valuable supplement to IM-MS due to the separation of ions in solution according to their size-to-charge ratio. We believe that KCE-MS will be used in parallel with circular dichroism (CD), stopped-flow (SF), and surface plasmon resonance (SPR) techniques for studying nucleic acid structures and functions, screening DNA/RNA binding compounds and selecting aptamers.

Experimental Section

Chemicals and reagents: All DNA sequences were purchased from IDT DNA Technologies (USA). For all experiments, 12.5 mM tris-acetate, pH 7.85, was used as an incubation/run buffer. The buffer was prepared by dilution from 200 mM tris-acetate stock buffer. The stock buffer was made by dissolving 12.11 g of tris-base (Bio Basic Inc., Canada, cat.# 77-86-1) and 2.86 mL of acetic acid (Bio Basic Inc., Canada, cat.# C1000) in 500 mL of ddH₂O. 100 mM solutions of NH₄Cl (Sigma-Aldrich, USA, cat.# 254134), NaCl (Sigma-Aldrich, USA, cat.# S7653) and KCl (Sigma-Aldrich, USA, cat.# P9541) were prepared in ddH₂O. 1 mM 4,4'-(propane-1,3-diyl)dibenzoic acid (PDDA; Sigma-Aldrich, USA, cat.# S49945) was prepared in run buffer and used as internal standard in CE separation to normalize electrophoretic mobilities.

Equilibrium mixtures of DNA and chlorides were prepared in the incubation buffer with 10 μ M concentration of all DNA sequences. Concentrations of KCl were in the range of 10 μ M–2.5 mM. All solu-

tions were filtered through 0.22 µm pore size nylon membrane filters (Millipore, Nepean, ON, Canada). The bare-silica capillary was purchased from Polymicro (Phoenix, AZ, USA).

KCE experiments: The sample storage and capillary temperature was maintained at $25 \pm 0.5^\circ\text{C}$. The electric field in KCE separation was 290 V cm^{-1} with a positive electrode at the injection end. The run buffer was with one of the coordinating ions in the inlet reservoir. The concentration of the coordinating ions in the equilibrium mixture and the run buffer was the same for individual KCE experiments. For all experiments, the capillary was 89 cm long (30 cm in KCE-UV experiment, 20 cm to window) with an inner diameter of 50 µm and an outer diameter of 360 µm. The equilibrium mixture was injected into the capillary from the inlet end by a pressure pulse of $10 \text{ s} \times 1 \text{ psi}$ (0.3 psi for 3 sec in KCE-UV experiment). Before each experiment, the capillary was rinsed by 75 psi pressure with: 0.1 M HCl for 3 min, 0.1 M NaOH for 3 min, ddH₂O for 3 min, 12.5 mM tris-acetate buffer for 5 min, and the incubation/run buffer with coordinating ions for 2 min. A Synapt G2 HDMS mass spectrometer from Waters (UK) was coupled with a PA800plus Pharmaceutical Analysis CE system having a PDA detector (Beckman Coulter, USA) through a CE-ESI sprayer from Micromass (UK) and used in all KCE-MS experiments. Electrospray ionization conditions were as follows: capillary voltage 3 kV, negative mode, sampling cone voltage 45 V, extraction cone voltage 3 V, source temperature 100°C , cone gas 0 L h^{-1} , nanoflow gas 0.5 Bar, purge gas 3 L h^{-1} , mobility cell bias voltage 3 V. Sheath liquid (80:20 isopropanol/ddH₂O, 5 mM triethanolamine) was delivered with a flow rate of $1.5 \mu\text{L min}^{-1}$.

Acknowledgements

This work was supported by the Natural Sciences and Engineering Research Council of Canada (grant RGPIN/385739–2010) and Canada Foundation for Innovation (project no. 25462). The authors also thank Dr. Jeffrey W. Keillor (University of Ottawa, Department of Chemistry) for providing a CD instrument and Justin Renaud (University of Ottawa, Department of Chemistry) for critical comments and valuable suggestions.

Keywords: capillary electrophoresis • DNA folding • G-quadruplexes • kinetics • mass spectrometry • structure characterization of biomolecules

- [1] Q. Wang, J. Q. Liu, Z. Chen, K. W. Zheng, C. Y. Chen, Y. H. Hao, Z. Tan, *Nucleic Acids Res.* **2011**, *39*, 6229.

- [2] T. Simonsson, P. Pecinka, M. Kubista, *Nucleic Acids Res.* **1998**, *26*, 1167.
- [3] J. X. Dai, D. Chen, R. A. Jones, L. H. Hurley, D. Z. Yang, *Nucleic Acids Res.* **2006**, *34*, 5133.
- [4] S. Rankin, A. P. Reszka, J. Huppert, M. Zloh, G. N. Parkinson, A. K. Todd, S. Ladame, S. Balasubramanian, S. Neidle, *J. Am. Chem. Soc.* **2005**, *127*, 10584.
- [5] S. Cogoi, F. Quadrifoglio, L. E. Xodo, *Biochemistry* **2004**, *43*, 2512.
- [6] D. Y. Sun, K. X. Guo, J. J. Rusche, L. H. Hurley, *Nucleic Acids Res.* **2005**, *33*, 6070.
- [7] D. Drygin, A. Siddiqui-Jain, S. O'Brien, M. Schwaebe, A. Lin, J. Bliesath, C. B. Ho, C. Proffitt, K. Trent, J. P. Whitten, J. K. C. Lim, D. Von Hoff, K. Andere, W. G. Rice, *Cancer Res.* **2009**, *69*, 7653.
- [8] M. J. Morris, Y. Negishi, C. Pazsint, J. D. Schonhoff, S. Basu, *J. Am. Chem. Soc.* **2010**, *132*, 17831.
- [9] S. Paramasivan, I. Rujan, P. H. Bolton, *Methods* **2007**, *43*, 324.
- [10] A. Y. Q. Zhang, S. Balasubramanian, *J. Am. Chem. Soc.* **2012**, *134*, 19297.
- [11] E. Henderson, C. C. Hardin, S. K. Walk, I. Tinoco, E. H. Blackburn, *Cell* **1987**, *51*, 899.
- [12] L. M. Ying, J. J. Green, H. T. Li, D. Klenerman, S. Balasubramanian, *Proc. Natl. Acad. Sci. USA* **2003**, *100*, 14629.
- [13] M. Adrian, B. Heddi, A. T. Phan, *Methods* **2012**, *57*, 11.
- [14] Y. Zhao, Z. Y. Kan, Z. X. Zeng, Y. H. Hao, H. Chen, Z. Tan, *J. Am. Chem. Soc.* **2004**, *126*, 13255.
- [15] N. H. Campbell, G. N. Parkinson, *Methods* **2007**, *43*, 252.
- [16] Y. Li, F. Xu, C. Liu, Y. Z. Xu, X. J. Feng, B. F. Liu, *Analyst* **2013**, *138*, 4475.
- [17] Y. Li, Y. Xu, X. Feng, B. F. Liu, *Anal. Chem.* **2012**, *84*, 9025.
- [18] J. A. Olivares, N. T. Nguyen, C. R. Yonker, R. D. Smith, *Anal. Chem.* **1987**, *59*, 1230.
- [19] A. Drabovich, M. Berezovski, S. N. Krylov, *J. Am. Chem. Soc.* **2005**, *127*, 11224.
- [20] A. Petrov, V. Okhonin, M. Berezovski, S. N. Krylov, *J. Am. Chem. Soc.* **2005**, *127*, 17104.
- [21] M. Berezovski, S. N. Krylov, *J. Am. Chem. Soc.* **2002**, *124*, 13674.
- [22] V. Okhonin, A. P. Petrov, M. Berezovski, S. N. Krylov, *Anal. Chem.* **2006**, *78*, 4803.
- [23] J. D. Cole, *Q. Appl. Math.* **1951**, *9*, 225.
- [24] E. Hopf, *Comm. Pure Appl. Math.* **1950**, *3*, 201.
- [25] G. G. Mironov, V. Okhonin, S. I. Gorelsky, M. V. Berezovski, *Anal. Chem.* **2011**, *83*, 2364.
- [26] M. U. Musheev, S. Javaherian, V. Okhonin, S. N. Krylov, *Anal. Chem.* **2008**, *80*, 6752.
- [27] E. S. Hong, H. J. Yoon, B. Kim, Y. H. Yim, H. Y. So, S. K. Shin, *J. Am. Soc. Mass Spectrom.* **2010**, *21*, 1245.
- [28] M. Vairamani, M. L. Gross, *J. Am. Chem. Soc.* **2003**, *125*, 42.
- [29] F. Balthasar, J. Plavec, V. Gabelica, *J. Am. Soc. Mass Spectrom.* **2013**, *24*, 1.
- [30] L. Z. Avila, Y. H. Chu, E. C. Blossey, G. M. Whitesides, *J. Med. Chem.* **1993**, *36*, 126.
- [31] Y.-H. Chu, L. Z. Avila, J. Gao, G. M. Whitesides, *Acc. Chem. Res.* **1995**, *28*, 461.

Received: January 29, 2014

Published online on April 2, 2014



Supporting Information

© 2014 The Authors. Published by Wiley-VCH Verlag GmbH & Co. KGaA, Weinheim

Conformational Dynamics of DNA G-Quadruplex in Solution Studied by Kinetic Capillary Electrophoresis Coupled On-line with Mass Spectrometry**

Gleb G. Mironov, Victor Okhonin, Nasrin Khan, Christopher M. Clouthier, and Maxim V. Berezovski*^[a]

[open_201400002_sm_miscellaneous_information.pdf](#)

Supporting Information

Cisplatin derivatization of GQ and GM. Experiments were performed with an excess and deficiency of cisplatin. Two incubation conditions were chosen: 20 minutes at 4°C and 12 h at 37°C. Monoderivatives of GQ and GM sequences (5 μ M each) with cisplatin were detected in trace amounts after 20 minutes at 4°C in the presence of 50 μ M cisplatin. After 12 h at 37°C, all DNA was derivatized with 2, 3, 4 cisplatin residues per DNA strand. In the presence of KCl the formation of GQ was observed only for the underivatized thrombin binding aptamer sequence.

Figure S1.2A shows that derivatized (GM-cisplatin) and non-derivatized (free GM) DNA travel with identical velocities and their peaks overlap completely. Thereby extracted spectrum for both peaks are identical. In the presence of 1 mM KCl (Fig. S1.2B) experimental results are identical due to the fact that GM sequences do not form a complex with K⁺ and do not fold into G-quadruplex structure. The same time propagation pattern is observed for GQ sequence in the absence of KCl (Fig. S1.2C). However, in the presence of 1 mM KCl there two peaks can be observed. As can be seen from extracted spectra, the first peak (green line) contains only derivatized GQ while the second peak (black line) contains only underivatized GQ. These results show that derivitazied GQ is not capable to fold into G-quadruplex,

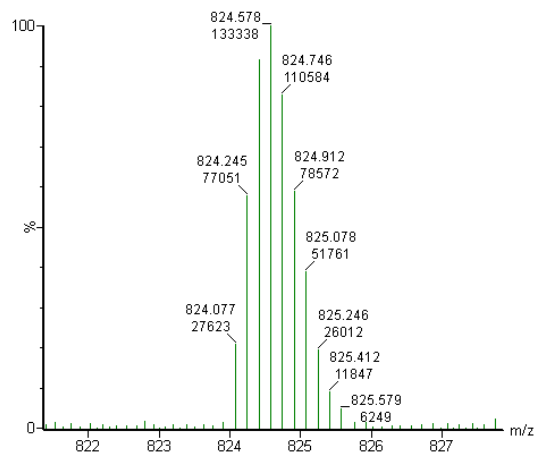


Figure S1.1. MS spectrum for GM-cisplatin complex.
Charge of the complex = -6.

while underivatized GQ fold into G-quadruplex and migrates slower in CE.

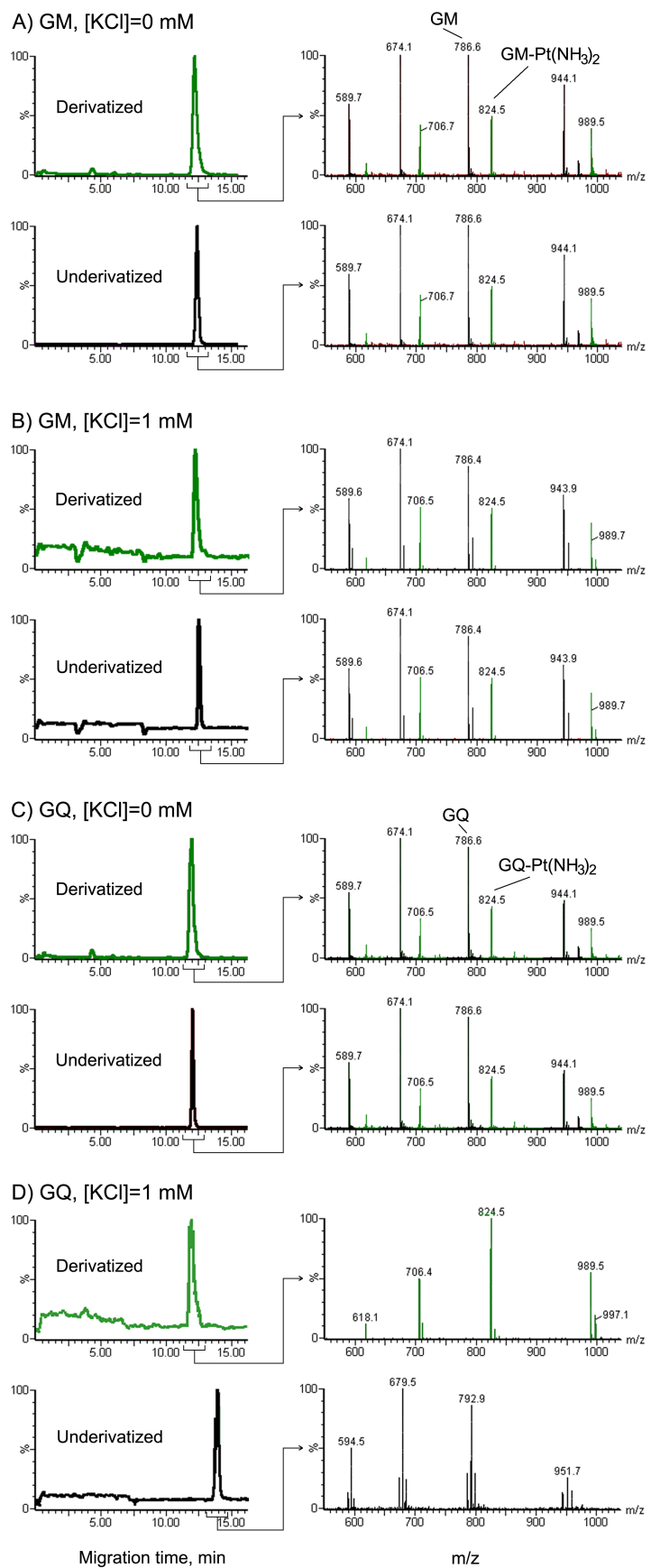


Figure S1.2. KCE-MS electropherograms and m/z ion spectra of GM and GQ sequences after cisplatin derivatization. Green color represents derivatized nucleic acid, black color represents underivatized nucleic acid.

Analytical Solution for Kinetics

Variables in the article and in the Supporting Information:

Article	Supporting Information
$[DNA]$	L
$[M]$	T
$[GQ-M]$	C
K_F	K_d

1. General mass transfer equations

Precise equations describing a binary reverse reaction happening during capillary electrophoresis - based separation are the following:

$$\frac{\partial L}{\partial t} + V_L \frac{\partial L}{\partial x} - D_L \frac{\partial^2 L}{\partial x^2} = \frac{\partial T_0}{\partial t} + V_T \frac{\partial T_0}{\partial x} - D_T \frac{\partial^2 T_0}{\partial x^2} = k_{off} C - k_{on} L T_0 = -\frac{\partial C}{\partial t} - V_C \frac{\partial C}{\partial x} + D_C \frac{\partial^2 C}{\partial x^2} \quad (0.1)$$

where L, T_0, C - concentrations of ligand, target and complex, respectively, V_L, V_T, V_C - electrophoretic velocities of these reactants, D_L, D_T, D_C - diffusion coefficients, t - time, x - a space coordinate, k_{off} - a decay rate constant, k_{on} - a rate constant of complex formation. Here, we start to discuss a special case of a sharp peak of the ligand and complex moving in a capillary with a initial concentration of target T . With the small difference between total concentration of the target and initial concentration ($\vartheta \equiv T_0 - T$), we have the following equations:

$$\frac{\partial L}{\partial t} + V_L \frac{\partial L}{\partial x} - D_L \frac{\partial^2 L}{\partial x^2} = \frac{\partial \vartheta}{\partial t} + V_T \frac{\partial \vartheta}{\partial x} - D_T \frac{\partial^2 \vartheta}{\partial x^2} = k_{off} C - k_{on} L (T + \vartheta) = -\frac{\partial C}{\partial t} - V_C \frac{\partial C}{\partial x} + D_C \frac{\partial^2 C}{\partial x^2} \quad (0.2)$$

These equations can be simplified in a few cases:

A. When the mobilities of the complex and the target are practically equal and diffusion coefficients play no significant role:

$$V_T = V_C, \quad D_T = D_C = D_L = 0 \quad (0.3)$$

For this case, using variable $P \equiv C + \vartheta$, we can obtain equations:

$$\begin{aligned} \frac{\partial P}{\partial t} + V_T \frac{\partial P}{\partial x} &= 0 \\ \frac{\partial L}{\partial t} + V_L \frac{\partial L}{\partial x} &= k_{off} (P - \vartheta) - k_{on} L (T + \vartheta) = \frac{\partial \vartheta}{\partial t} + V_T \frac{\partial \vartheta}{\partial x} \end{aligned} \quad (0.4)$$

Further simplification can be made by using Cole-Hopf transformation. New variable w is connected with initial variables by the expression:

$$L = \frac{\partial w}{\partial t} + V_T \frac{\partial w}{\partial x}, \quad \vartheta = \frac{\partial w}{\partial t} + V_L \frac{\partial w}{\partial x} \quad (0.5)$$

where w can be described as:

$$\left(\left(\frac{\partial}{\partial t} + V_L \frac{\partial}{\partial x} \right) \left(\frac{\partial}{\partial t} + V_T \frac{\partial}{\partial x} \right) + k_{off} \left(\frac{\partial}{\partial t} + V_L \frac{\partial}{\partial x} \right) + k_{on} T \left(\frac{\partial}{\partial t} + V_T \frac{\partial}{\partial x} \right) - k_{off} P \right) \exp(k_{on} w) = 0 \quad (0.6)$$

B. This is the case of big decay constant k_{off} and weak nonlinearity, when target concentration is changed slowly by the ligand and complex, $|\vartheta| = T$. Diffusion coefficients are not zero but small. In this case, the equations can be rewritten as:

$$\frac{\partial(L+C)}{\partial t} + \frac{\partial(V_L L + V_C C)}{\partial x} = \frac{\partial^2(D_L L + D_C C)}{\partial x^2}, \quad C = \frac{1}{1 + \frac{1}{k_{off}} \left(\frac{\partial}{\partial t} + V_C \frac{\partial}{\partial x} - D_C \frac{\partial^2}{\partial x^2} \right)} L \frac{T + \vartheta}{K_d} \quad (0.7)$$

$$\vartheta = \left(1 + \frac{(V_L - V_T) \frac{\partial}{\partial x} - (D_L - D_T) \frac{\partial^2}{\partial x^2}}{\frac{\partial}{\partial t} + V_T \frac{\partial}{\partial x} - D_T \frac{\partial^2}{\partial x^2}} \right) L$$

In the first order by small values, it can be simplified to:

$$C \approx T \frac{L}{K_d} - \frac{T}{k_{off} K_d} \left(\frac{\partial}{\partial t} + V_C \frac{\partial}{\partial x} - D_C \frac{\partial^2}{\partial x^2} \right) L + \frac{\vartheta L}{K_d}, \quad \vartheta \approx \left(1 + \frac{(V_L - V_T) \frac{\partial}{\partial x}}{\frac{\partial}{\partial t} + V_T \frac{\partial}{\partial x}} \right) L \quad (0.8)$$

$$\frac{\partial L}{\partial t} \left(1 + \frac{T}{K_d} \right) + \frac{\partial \left(V_L + V_C \frac{T}{K_d} \right) L}{\partial x} + \left(\frac{\partial}{\partial t} + V_C \frac{\partial}{\partial x} \right) \frac{\vartheta L}{K_d} \approx \left(\frac{\partial^2 \left(D_L + D_C \frac{T}{K_d} \right)}{\partial x^2} + \frac{T}{k_{off} K_d} \left(\frac{\partial}{\partial t} + V_C \frac{\partial}{\partial x} \right)^2 \right) L$$

By introducing new variables:

$$V_{EM} = \frac{V_L K_d + V_C T}{K_d + T}, D_{EM} = \frac{D_L K_d + D_C T}{K_d + T} \quad (0.9)$$

and, using the approximate expression that is correct in the zero order:

$$\frac{\partial}{\partial t} \approx -V_{EM} \frac{\partial}{\partial x} \quad (0.10)$$

We can finally obtain:

$$\left(\frac{\partial L}{\partial t} + V_{EM} \frac{\partial L}{\partial x} \right) + \frac{(V_C - V_{EM})(V_L - V_{EM})}{(V_T - V_{EM})(K_d + T)} \frac{\partial}{\partial x} L^2 \approx \left(D_{EM} + \frac{T(V_C - V_{EM})^2}{k_{off}(K_d + T)} \right) \frac{\partial^2}{\partial x^2} L \quad (0.11)$$

In addition:

$$C \approx T \frac{L}{K_d} - \frac{T(V_C - V_{EM})}{k_{off} K_d} \frac{\partial L}{\partial x} + \frac{L^2}{K_d} \frac{V_L - V_{EM}}{V_T - V_{EM}}, \quad \vartheta \approx \frac{V_L - V_{EM}}{V_T - V_{EM}} L \quad (0.12)$$

For the summarized concentration of ligand and complex $P \equiv L + C$, the equation is following:

$$L \approx \frac{K_d}{K_d + T} P + \frac{TK_d(V_C - V_{EM})}{k_{off}(K_d + T)^2} \frac{\partial}{\partial x} P + \frac{P^2 K_d^2}{(K_d + T)^3} \frac{V_L - V_{EM}}{V_T - V_{EM}} \quad (0.13)$$

$$\left(\frac{\partial}{\partial t} + V_{EM} \frac{\partial}{\partial x} \right) P + \frac{K_d(V_C - V_{EM})(V_L - V_{EM})}{(V_T - V_{EM})(K_d + T)^2} \frac{\partial}{\partial x} P^2 \approx \left(D_{EM} + \frac{T(V_C - V_{EM})^2}{k_{off}(K_d + T)} \right) \frac{\partial^2}{\partial x^2} P$$

Equation (0.13) can be rewritten using expressions for their coefficients:

$$G = \frac{K_d(V_C - V_{EM})(V_L - V_{EM})}{(V_T - V_{EM})(K_d + T)^2} = \frac{TK_d^2(V_C - V_L)^2}{(V_{EM} - V_T)(K_d + T)^4} \quad (0.14)$$

$$D_{CID} = \frac{T(V_C - V_{EM})^2}{k_{off}(K_d + T)} = \frac{TK_d^2(V_C - V_L)^2}{k_{off}(K_d + T)^3}$$

Finally:

$$\left(\frac{\partial}{\partial t} + V_{EM} \frac{\partial}{\partial x} \right) P + G \frac{\partial}{\partial x} P^2 \approx (D_{EM} + D_{CID}) \frac{\partial^2}{\partial x^2} P \quad (0.15)$$

This equation can be transformed into a linear diffusion equation using standard Cole-Hopf transformation:

$$P(x, t) = -\frac{\partial}{\partial x} \frac{D_{EM} + D_{CID}}{G} \ln \left(\Theta_0 + \int_{-\infty}^x Q(x', t) dx' \right), \quad (0.16)$$

$$Q(x, t) = \frac{\partial}{\partial x} \exp \left(\frac{-G}{D_{EM} + D_{CID}} \int_{-\infty}^x P(x', t) dx' \right)$$

For Cole-Hopf variable Q , a linear equation is satisfied:

$$\left(\frac{\partial}{\partial t} + V_{EM} \frac{\partial}{\partial x} \right) Q \approx (D_{EM} + D_{CID}) \frac{\partial^2}{\partial x^2} Q \quad (0.17)$$

2. Partial solutions

The simplest solution of the equation (0.17) has a form:

$$Q : Q_0 + \frac{1}{\sqrt{\pi(\Delta_0^2 + 4t(D_{EM} + D_{CID}))}} \exp \left(-\frac{(x - V_{EM}t)^2}{\Delta_0^2 + 4t(D_{EM} + D_{CID})} \right) \quad (1.1)$$

The total concentration of bound and free ligand after Cole-Hopf transformation is corresponded to:

$$P(x, t) = \frac{D_{EM} + D_{CID}}{|G|\Delta} \frac{\exp \left(-\frac{(x - V_{EM}t)^2}{\Delta} \right)}{\left| \sqrt{\pi} B + \int_{-\infty \cdot sign(V_T - V_{EM})}^{\frac{(x - V_{EM}t)}{\Delta}} \exp(-x^2) dx \right|} =$$

$$= \frac{\left(1 + \frac{D_{EM}}{D_{CID}} \right) (K_d + T) |V_T - V_{EM}|}{k_{off}\Delta} \frac{\exp \left(-\left(\frac{x - V_{EM}t}{\Delta} \right)^2 \right)}{\left| \sqrt{\pi} B + \int_{-\infty \cdot sign(V_T - V_{EM})}^{\frac{(x - V_{EM}t)}{\Delta}} \exp(-x^2) dx \right|} \quad (1.2)$$

where Δ is defined as:

$$\Delta \equiv \sqrt{\Delta_0^2 + 4t(D_{EM} + D_{CID})} \quad (1.3)$$

The total amount of bounded and free ligand $L_0 \times l$ per unit of a capillary section area is:

$$L_0 \times l = \int_{-\infty}^{\infty} P(x) dx = \frac{1}{k_{off}} \left(1 + \frac{D}{D_{CID}} \right) (K_d + T) |V_T - V| \ln \left(1 + \frac{1}{B} \right) \quad (1.4)$$

According (1.4),

$$B = 1 / \left(\exp \left(\frac{k_{off} D_{CID} L_0 \times l}{|V_T - V| (K_d + T) (D_{CID} + D)} \right) - 1 \right) \quad (1.5)$$

3. Initial conditions

Initial condition corresponds to a rectangular plug with length, l , and the sum concentration of the ligand and complex, L_0 . After Cole – Hopf transformation (0.16) the initial condition for equation (0.17) has a form:

$$Q(x, 0) = -\frac{GL_0 \theta(x) \theta(l-x)}{D_{EM} + D_{CID}} \exp \left(\frac{-GL_0 x}{D_{EM} + D_{CID}} \right) \quad (3.1)$$

Mean square of coordinates for distribution (3.1) is

$$2 \langle \delta x^2 \rangle = 2 \left(\frac{l}{\lambda} \right)^2 \left(\frac{\int_0^\lambda \exp(x) x^2 dx}{\int_0^\lambda \exp(x) dx} - \left(\frac{\int_0^\lambda \exp(x) x dx}{\int_0^\lambda \exp(x) dx} \right)^2 \right) \quad (3.2)$$

where λ is defined as:

$$|\lambda| = \left| \frac{GL_0 \times l}{D_{EM} + D_{CID}} \right| = \left| \frac{k_{off} L_0 \times l}{(1 + D_{EM} / D_{CID})(K_d + T)(V_T - V_{EM})} \right| \quad (3.3)$$

equation (3.2) can be transformed as

$$2 \langle \delta x^2 \rangle = 2 \left(\frac{l}{\lambda} \right)^2 \left(1 - \left(\frac{\lambda/2}{\sinh(\lambda/2)} \right)^2 \right) \quad (3.4)$$

According to (0.17), value (3.4) is equal to value Δ_0^2 in expressions (1.1) and (1.3). Mean square of coordinates in diffusion process always depends on time exactly the same as for Gaussian peaks, and an every peak becomes near Gaussian with time. Finally, for Δ_0 we can have:

$$\Delta_0 = \sqrt{2} \left| \frac{l}{\lambda} \right| \sqrt{1 - \left(\frac{\lambda/2}{\sinh(\lambda/2)} \right)^2} \quad (3.5)$$

4. Peaks fitting

According to(1.2), the form of a peak in an electropherogram can be described as:

$$\rho(t) = \frac{A \exp(-(t-t_0)^2/w^2)}{w \left| \sqrt{\pi} B + \int_{-\infty \cdot sign(V_T - V_{EM})}^{(t-t_0)/w} \exp(-x^2) dx \right|} \quad (4.1)$$

We need to know parameters t_0 , A , w and $J \equiv \ln\left(1 + \frac{1}{|B|}\right)$ for proper describing the form of the peak. The direct way to determine these parameters is the fitting the form of the peak.

We can also find these parameters without peak fitting by following steps:

1. A can be found from the expression:

$$A = \int_{-\infty}^{\infty} \rho(t) dt \quad (4.2)$$

2. For a sharp peak, t_0 corresponds to peak's maximum. It becomes precise for big enough B , but possible imprecision play no practical role. This parameter is in use for K_d determination, and possible relative error as a result of imprecision is not higher the ratio of peak width on the electropherogram to t_0 .

3. For big B what means small J , parameter w can be found from expression

$$w = \sqrt{2\langle \delta t^2 \rangle} \quad (4.3)$$

For arbitrary B , (4.3) can be generalized to expression

$$w = \sqrt{2\langle \delta t^2 \rangle / \Phi(J(B))} \quad (4.4)$$

where function $\Phi(J)$ is defined by the expressions:

$$\Phi(B) = \sqrt{\frac{\int_{-\infty}^{\infty} \tau^2 \rho(\tau) d\tau}{\int_{-\infty}^{\infty} \rho(\tau) d\tau}} - \left(\frac{\int_{-\infty}^{\infty} \tau \rho(\tau) d\tau}{\int_{-\infty}^{\infty} \rho(\tau) d\tau} \right)^2 \quad (4.5)$$

where

$$\rho(\tau) = \frac{\partial}{\partial \tau} \ln \left(\sqrt{\pi} |B| + \int_{-\infty}^{\tau} \exp(-x^2) dx \right) \quad (4.6)$$

The approximate expression for the function $\Phi(J)$ can be found numerically and has a form:

$$\Phi(J) \approx (1 + J^{1.88159722011194} / 31.8307184800561)^{0.23611765995013} \quad (4.7)$$

4. For finding peak's asymmetry, J , a ratio of peak's subareas before and after its maximum can be used. For expression (4.6) describing the shape of the peak, the position of peak's maximum, z , is satisfied to the following equation:

$$\partial_z \rho(z) = -(2z + \rho(z)) \rho(z) = 0 \Rightarrow 2z + \rho(z) = 0 \quad (4.8)$$

According to (4.6) and (4.8)

$$\frac{\exp(-z^2)}{2z} + \int_{-\infty}^z \exp(-y^2) dy = -B\sqrt{\pi} \quad (4.9)$$

Subareas are integrals of (4.6) before and after z . The ratio of a bigger subarea to smaller subarea, r , can be expressed as a function of J :

$$r = \frac{J}{\ln \left(1 + \frac{\exp(J) - 1}{\sqrt{\pi}} \int_{-\infty}^z \exp(-y^2) dy \right)} - 1 \quad (4.10)$$

Based on (4.10), the approximated connection between J and r can be found as:

$$J \approx 5.49902754 \cdot (r-1)^{0.879250897} \cdot \exp((r-1) \cdot 0.028860911) \quad (4.11)$$

5. Constants determinations

According to (4.1), if two peaks are different only by their widths and asymmetries, then the square difference between them will be

$$\begin{aligned} H(w_1, B_1, w_2, B_2) &= \int \left(\frac{\rho(t, t_0, A, w_1, B_1)}{\int_{-\infty}^{\infty} \rho(t', t_0, A, w_1, B_1) dt'} - \frac{\rho(t, t_0, A, w_2, B_2)}{\int_{-\infty}^{\infty} \rho(t', t_0, A, w_2, B_2) dt'} \right)^2 dt = \\ &= \int \left(\frac{\partial}{\partial t} \left(\frac{\ln \left(\sqrt{\pi} B_1 + \int_{-\infty}^{t/w_1} \exp(-x^2) dx \right)}{\ln(1+1/B_1)} - \frac{\ln \left(\sqrt{\pi} B_2 + \int_{-\infty}^{t/w_2} \exp(-x^2) dx \right)}{\ln(1+1/B_2)} \right) \right)^2 dt \end{aligned} \quad (5.1)$$

Expression (5.1) can be simplified when we define new variables:

$$w = (w_1 + w_2)/2, \quad B = (B_1 + B_2)/2, \quad \delta w = (w_1 - w_2)/2, \quad \delta B = (B_1 - B_2)/2 \quad (5.2)$$

And assume that difference between parameters δw and δB is small:

$$\begin{aligned} N &\equiv \sqrt{\pi} B + \int_{-\infty}^z \exp(-x^2) dx, \quad F \equiv \frac{\exp(-z^2)}{N}, \quad J \equiv \ln \left(1 + \frac{1}{B} \right) \\ H &\approx \frac{4}{w} \int \left(\left(\frac{\partial}{\partial z} \frac{\left(\sqrt{\pi} \delta B - \frac{z \delta w}{w} \exp(-z^2) \right)}{NJ} + \frac{\delta B F}{B^2 J^2} \right) \right)^2 dz = \\ &= \frac{4}{w J^2} \int \left(F \left(\frac{\delta w}{w} \left(1 - 2z^2 - zF \right) + \delta B \left(\frac{\sqrt{\pi}}{N} - \frac{1}{B^2 J} \right) \right) \right)^2 dz = \\ &\equiv I_0(J) \frac{\delta J^2}{w} + I_1(J) \frac{\delta w}{w^2} \delta J + I_2(J) \frac{\delta w^2}{w^3} \end{aligned} \quad (5.3)$$

where parameter B is connected with the asymmetry parameter J :

$$B = \frac{1}{\exp(J)-1}, \quad \delta B = -\frac{\delta J}{4 \sinh(J/2)^2} \quad (5.4)$$

And used for definitions:

$$I_0(J) \equiv \frac{1}{4J^2 \sinh(J/2)^4} \int \left(F\left(\frac{\sqrt{\pi}}{N} - \frac{1}{B^2 J}\right) \right)^2 dz \quad (5.5)$$

$$I_2(J) \equiv \frac{4}{J^2} \int \left(F(1 - 2z^2 - zF) \right)^2 dz$$

$$I_1(J) \equiv \frac{-2}{J^2 \sinh(J/2)^2} \int F\left(\frac{\sqrt{\pi}}{N} - \frac{1}{B^2 J}\right) F(1 - 2z^2 - zF) dt$$

Integrals (5.5) can be found numerically, as functions of J , so approximate expressions for them are

$$I_0(J) \approx \exp(-1.2528245054 + 0.4458595661 \cdot J + 0.0783120873 \cdot J^2 - 0.0014341015 \cdot J^3)$$

$$I_1(J) \approx \exp(-1.5332457793 - 0.0255243875 \cdot J + 0.0472953261 \cdot J^2 - 0.0008175906 \cdot J^3) \quad (5.6)$$

$$I_2(J) \approx \exp(-1.8876358911 - 0.6609871055 \cdot J + 0.0300281253 \cdot J^2 - 0.0005155394 \cdot J^3)$$

For fitting of the parameters, total error for few experiments will be sum of the approximated expressions (5.3).

6. Confidence of the data in different experimental conditions

Variations of width and asymmetry are connected with variation k_{off} according the following expressions:

$$\delta J = J \frac{\delta k_{off}}{k_{off}}, \quad \delta w = -\frac{2tD_{CID}}{w} \frac{\delta k_{off}}{k_{off}} \quad (6.1)$$

Based on (6.1), (5.3) can be rewriting in the form of:

$$H = S \cdot \left(\frac{\delta k_{off}}{k_{off}} \right)^2, \quad S = I_0(J) \frac{J^2}{w} - I_1(J) \frac{2tJD_{EM}}{w^3} + I_2(J) \frac{4(tD_{EM})^2}{w^5} \quad (6.2)$$

where S is confidence of the data. In **Figure S2**, the typical behavior of the confidence for GQ-M complex formation is presented.

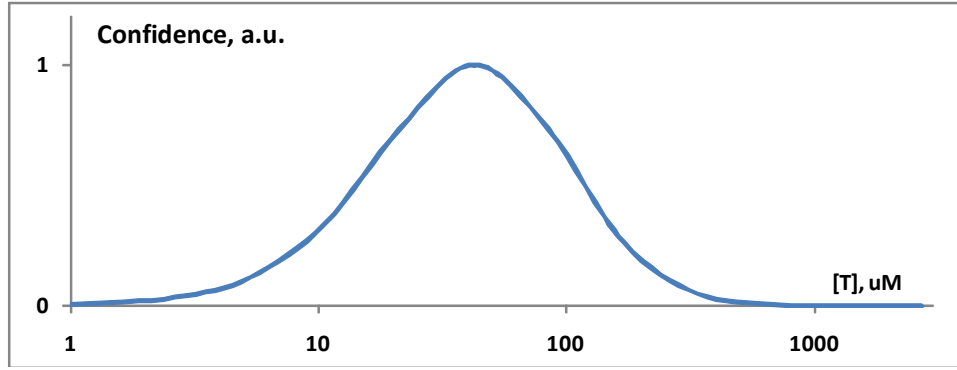


Figure S2. The behavior of the confidence for GQ-M complex formation.

7. K_d determination based on a set of experiments

According (0.9) K_d can be determined from single experiment:

$$K_d \approx T \frac{V_C - V_{EM}}{V_{EM} - V_L} \quad (7.1)$$

If we have a set of experiments, with different target concentrations, and errors of velocity measurements are similar for all experiments, then can be found by minimization expression

$$\sum_i \left(V_{EM}^i - \frac{V_L K_d + V_C T^i}{K_d + T^i} \right)^2 \quad (7.2)$$

The minimum can be found numerically. Also, it can be used approximate expression. To get it, we can start from differential condition for extreme (7.2) as a function of K_d :

$$K_d \approx \sum_i \frac{(V_C - V_{EM}^i)(T^i)^2}{(K_d + T^i)^3} / \sum_i \frac{(V_{EM}^i - V_L)T^i}{(K_d + T^i)^3} \quad (7.3)$$

Which is a nonlinear equation for K_d . To simplify it, we can approximately use(7.1), to estimate

$$(K_d + T^i)^3 \approx (T^i)^3 \left(\frac{V_C - V_L}{V_{EM} - V_L} \right)^3 \quad (7.4)$$

Which after substituting into right part of (7.3) gives:

$$K_d \approx \sum_i \frac{(V_i^{EM} - V_L)^3 (V_C - V_i^{EM})}{T_i} / \sum_i \frac{(V_i^{EM} - V_L)^4}{T_i^2} \quad (7.5)$$

8. K_d determination for complex stoichiometry.

If complex contains more than one (n) targets, instead(0.9), according, can be used expression

$$V_{EM} \equiv \frac{V_L K_d + V_C T^n}{K_d + T^n} \quad (8.1)$$

In this case K_d can be determined from single experiment:

$$K_d \approx T^n \frac{V_C - V_{EM}}{V_{EM} - V_L} \quad (8.2)$$

or from the set of experiments:

$$K_d \approx \sum_i \frac{(V_i^{EM} - V_L)^3 (V_C - V_i^{EM})}{T_i^n} / \sum_i \frac{(V_i^{EM} - V_L)^4}{T_i^{2n}} \quad (8.3)$$

Analogously, the approach for k_{off} determination also can be generalized on the case of this stoichiometry.

Circular Dichroism experiments

Experimental conditions: instrument Jasco J815 CD (Jasco Inc., USA), data interval 0.1 nm, cell length 1 mm, temperature 25°C, scanning speed 100 nm/min, concentration of GQ 10 μ M, 12.5 mM Tris-Acetate buffer. K_D value was calculated using Scatchard plot and GRG nonlinear engine solver in Microsoft Excel 2010.

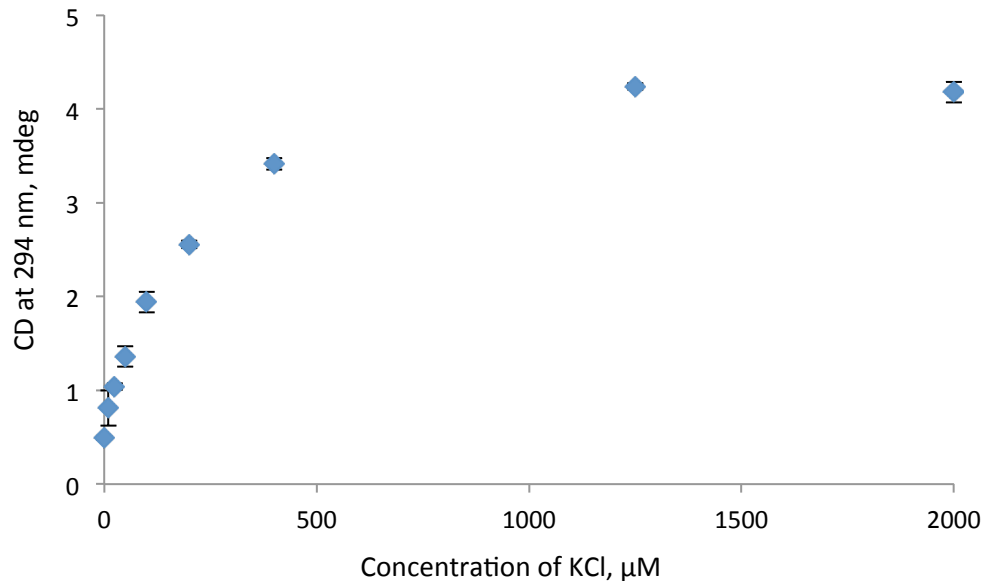


Figure S3. Plot of CD spectra at 294 nm as a function of KCl concentrations.

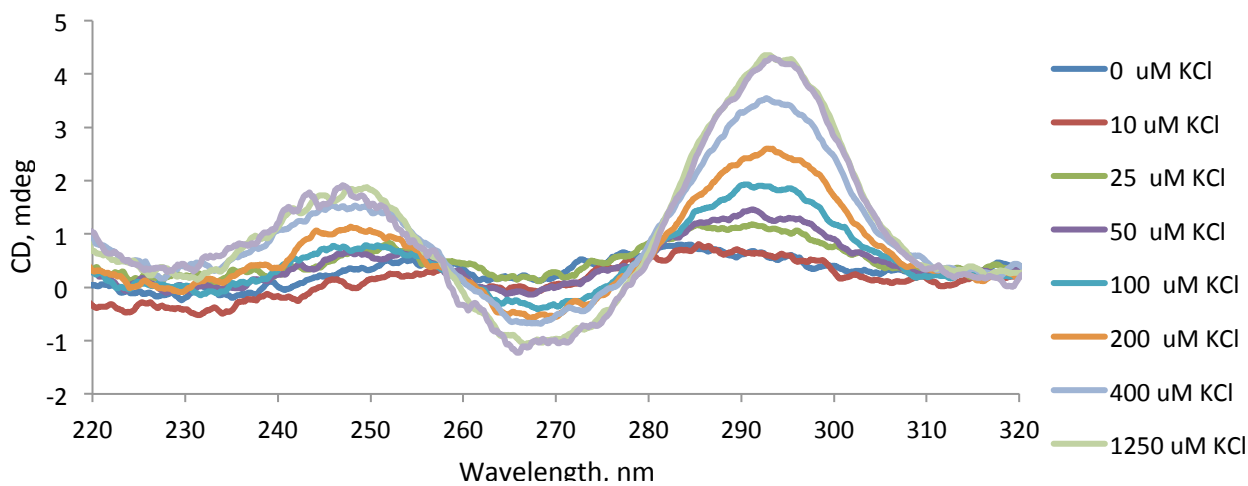


Figure S4. CD spectra of GQ sequence at different concentrations of KCl.